

Task-Agnostic Learning to Accomplish New Tasks

Xianqi Zhang, Xingtao Wang, Xu Liu, Wenrui Wang, Xiaopeng Fan, *Senior Member, IEEE*,
and Debin Zhao, *Member, IEEE*

Abstract—Reinforcement Learning (RL) and Imitation Learning (IL) have made great progress in robotic control in recent years. However, these methods show obvious deterioration for new tasks that need to be completed through new combinations of actions. RL methods heavily rely on reward functions that cannot generalize well for new tasks, while IL methods are limited by expert demonstrations which do not cover new tasks. In contrast, humans can easily complete these tasks with the fragmented knowledge learned from task-agnostic experience. Inspired by this observation, this paper proposes a task-agnostic learning method (TAL for short) that can learn fragmented knowledge from task-agnostic data to accomplish new tasks. TAL consists of four stages. First, the task-agnostic exploration is performed to collect data from interactions with the environment. The collected data is organized via a knowledge graph. Compared with the previous sequential structure, the knowledge graph representation is more compact and fits better for environment exploration. Second, an action feature extractor is proposed and trained using the collected knowledge graph data for task-agnostic fragmented knowledge learning. Third, a candidate action generator is designed, which applies the action feature extractor on a new task to generate multiple candidate action sets. Finally, an action proposal is designed to produce the probabilities for actions in a new task according to the environmental information. The probabilities are then used to select actions to be executed from multiple candidate action sets to form the plan. Experiments on a virtual indoor scene show that the proposed method outperforms the state-of-the-art offline RL method: CQL by 35.28% and the IL method: BC by 22.22%.

Index Terms—Robotic manipulation, task-agnostic learning, knowledge graph, action feature extraction, machine learning.

I. INTRODUCTION

A Robot is expected to learn and work in the same way that humans do. To this end, Reinforcement Learning (RL) and Imitation Learning (IL) are proposed and developed. In reality, there are always new tasks that must be completed through new combinations of actions. For example, “reading a book” needs “turn on the light and push the chair near the table” to perform. Actions such as “turn on the light” and “push the chair near the table” may have been done before independently, but not sequentially together. Humans can easily complete these new tasks, but it is very challenging for RL and IL methods.

RL has made significant advances in robotics applications [1]–[9]. Reward functions play a crucial role in RL. For example, Hadfield *et al.* [10] introduced the approximate method

for solving the inverse reward design problem. He *et al.* [11] proposed an assisted reward design method that accelerates the design process. In addition, some works aim to alleviate the data distributional shift problem [12], i.e., the agent cannot perform well when training and testing data differ significantly. For example, Kumar *et al.* [13] proposed Conservative Q-Learning (CQL), where they used a Q-value regularizer to constrain the learned Q-function. Yu *et al.* [14] proposed Conservative Offline Model-Based Policy Optimization (COMBO) to learn a conservative Q-function. In general, RL methods heavily rely on reward functions that cannot generalize well for new tasks, since reward functions are typically task-specific. Furthermore, when processing new tasks, the distribution shift problem may be more serious, making the generalization of the reward function more difficult.

IL refers to making a robot imitate the behavior of experts [15]–[20]. IL methods need to collect expert demonstrations in advance and teach the agent to imitate the expert behavior to achieve the goal [17]. Finn *et al.* [18] employed neural networks for learning cost functions to enable an agent to mimic expert activities. Ho *et al.* [19] utilized the idea of generative adversarial and proposed Generative Adversarial Imitation Learning (GAIL). Torabi *et al.* [20] proposed Behavioral Cloning from Observation (BCO) to enable the agent to learn from the state-only demonstration. Ehsani *et al.* [21] trained a model to mimic the activities of the characters in videos. However, IL methods are limited by expert demonstrations which do not cover new tasks, making their performance deteriorate.

In contrast, humans can easily complete these new tasks with the fragmented knowledge learned from task-agnostic experience. An important way for humans to learn fragmented knowledge is to learn from task-agnostic interactions with environments. For example, when a child interacts with objects in the environment without a specific goal in mind, he/she may learn fragmented knowledge such as “a block can be picked up” or “some blocks can be combined in a certain way.” To complete a new task, a child first roughly estimates the actions required to complete the task according to the fragmented knowledge, and then determines the execution order of the actions based on the environmental state. For example, to construct a desired shape, a child will estimate the required blocks and then combine them in a certain order.

In this paper, inspired by how humans handle new tasks, i.e., learn the fragmented knowledge → select the actions that will be used for a new task → decide the action order to be executed, we propose a task-agnostic learning method (TAL for short) that can learn fragmented knowledge from task-agnostic data to accomplish new tasks. TAL contains four stages: task-agnostic environment exploration, action feature extraction,

X. Zhang, X. Wang, X. Liu, W. Wang, X. Fan, and D. Zhao are with the Research Center of Intelligent Interface and Human Computer Interaction, the Department of Computer Science and Technology, Harbin Institute of Technology, Harbin 150001, China. E-mail: zhangxianqi@stu.hit.edu.cn; xtwang@hit.edu.cn; 20B903008@stu.hit.edu.cn; 21B303001@stu.hit.edu.cn; fxp@hit.edu.cn; dbzhao@hit.edu.cn.

Corresponding author: Xiaopeng Fan.

Project page: https://xianqi-zhang.github.io/Learn_From_Task-Agnostic/

candidate action generation, and plan generation by action proposal. Compared with RL and IL methods, TAL overcomes the limitations of reward functions and expert demonstrations, making it more suitable to accomplish new tasks.

The main contributions of this paper are summarized as follows:

- A task-agnostic learning method (TAL for short) is proposed, which can learn fragmented knowledge from task-agnostic data to accomplish new tasks.
- The task-agnostic exploration is performed to collect data which is organized via a knowledge graph. Compared with the previous sequential structure, the knowledge graph representation is more compact and fits better for environment exploration.
- An action feature extractor is proposed and trained using the collected knowledge graph data for task-agnostic fragmented knowledge learning.
- A candidate action generator is proposed, which applies the action feature extractor on a new task to generate multiple candidate action sets.
- An action proposal is designed to produce the probabilities for actions in a new task according to the environmental information. The probabilities are then used to select actions to be executed from multiple candidate action sets to form the plan.

The rest of this paper is organized as follows. Related works are briefly reviewed in Section II. The proposed framework is described in Section III. The experimental results are presented in Section IV. Section V provides the conclusion.

II. RELATED WORK

A. Reinforcement Learning

Reinforcement Learning (RL) has been widely used in robotics-related scenarios [1]–[9]. Mnih *et al.* [22] proposed Deep Q-Network (DQN), which first combined CNN and Q-learning to play Atari games and achieved human-level performance. Lillicrap *et al.* [23] proposed Deep Deterministic Policy Gradient (DDPG) to operate over continuous action spaces. Fujimoto *et al.* [24] proposed Batch-Constrained deep Q-learning (BCQ) to force the agent to better learn from offline data by restricting the action space. Besides, goal-conditioned RL is proposed to enable an agent to be able to perform multiple tasks [25]–[31]. The agent is anticipated to consider both task and environmental information when making decisions [28], [29].

Reward functions play a crucial role in RL. Hadfield *et al.* [10] introduced the approximate method for solving the inverse reward design (IRD) problem. Devidze *et al.* [32] proposed a new framework to investigate the explicable reward function design from the perspective of discrete optimization. Their framework captures the (sub-)optimality of target policies at different time horizons in terms of actions taken from any given starting state. He *et al.* [11] proposed an assisted reward design method that accelerates the design process by anticipating and influencing future design iterations.

In addition, some works aim to alleviate the data distributional shift problem [12], i.e., the agent cannot perform well

when training and testing data differ significantly. To alleviate this problem, Kumar *et al.* [13] proposed Conservative Q-Learning (CQL), where they used a Q-value regularizer to constrain the learned Q-function. Yu *et al.* [14] proposed Conservative Offline Model-Based Policy Optimization (COMBO) to learn a conservative Q-function by penalizing the value function on out-of-support state-action tuples. Wiles *et al.* [33] analyzed the distributional shift problem in detail and gave some suggestions, such as data augmentation and pre-training.

RL methods heavily rely on reward functions that cannot generalize well for new tasks, since the reward function is typically task-specific. Furthermore, when processing new tasks, the distribution shift problem may be more serious, making the generalization of the reward function more difficult.

B. Imitation Learning

Imitation Learning (IL), also known as learning from demonstration, refers to making a robot imitate the behavior of experts [34]–[36].

A branch of the IL method is Inverse Reinforcement Learning (IRL), which seeks to recover reward function from demonstrations. Finn *et al.* [18] employed neural networks for learning cost function and combined IRL to teach the agent to carry out identical activities as the expert. Ho *et al.* [19] proposed a new framework called Generative Adversarial Imitation Learning (GAIL), which combined IRL with the idea of generative adversarial, and gained remarkable performance and widespread attention [37]–[41].

Another branch is Behavioral Cloning (BC), which aims to mimic expert behavior through supervised learning. With the great progress of Deep Learning (DL), many works use DL to manipulate a robot. Finn and Levine [42] proposed a deep predictive model for object manipulation tasks. Their research reveals that using a predictive model for robot control is practical. Agrawal *et al.* [43] proposed a CNN-based model to enable the agent to prod the object into the desired position. In these two works, only one camera is equipped in the head of a robot, overlooking the desktop environment. Although it takes place in a 3D real-world setting, the essence is still to translate into a 2D space for reasoning and planning. Recently, the combination of BC and DL has attracted extensive attention. Torabi [20] proposed Behavioral Cloning from Observation (BCO) to enable the agent to learn from the state-only demonstration. Edwards *et al.* [44] proposed Imitating Latent Policies from Observation (ILPO) to infer latent policies directly from state observations. In the physics simulator Pybullet [45], Ehsani *et al.* [21] trained a model to mimic the activities of humans in videos. But most of the actions imitated are translations or rotations with only one object present in the scene. Sharma *et al.* [46] trained two models, in which the high-level model generated a series of first-person sub-goals based on the video from the third-person perspective, and the low-level model predicted the actions necessary to fulfill the sub-goals. This paradigm is similar to hierarchical RL [47]–[52]. In addition, to alleviate the difficulty of collecting expert demonstrations, Lynch *et al.* [53] let humans manipulate robots to collect task-agnostic data and call it play data. Since there is no

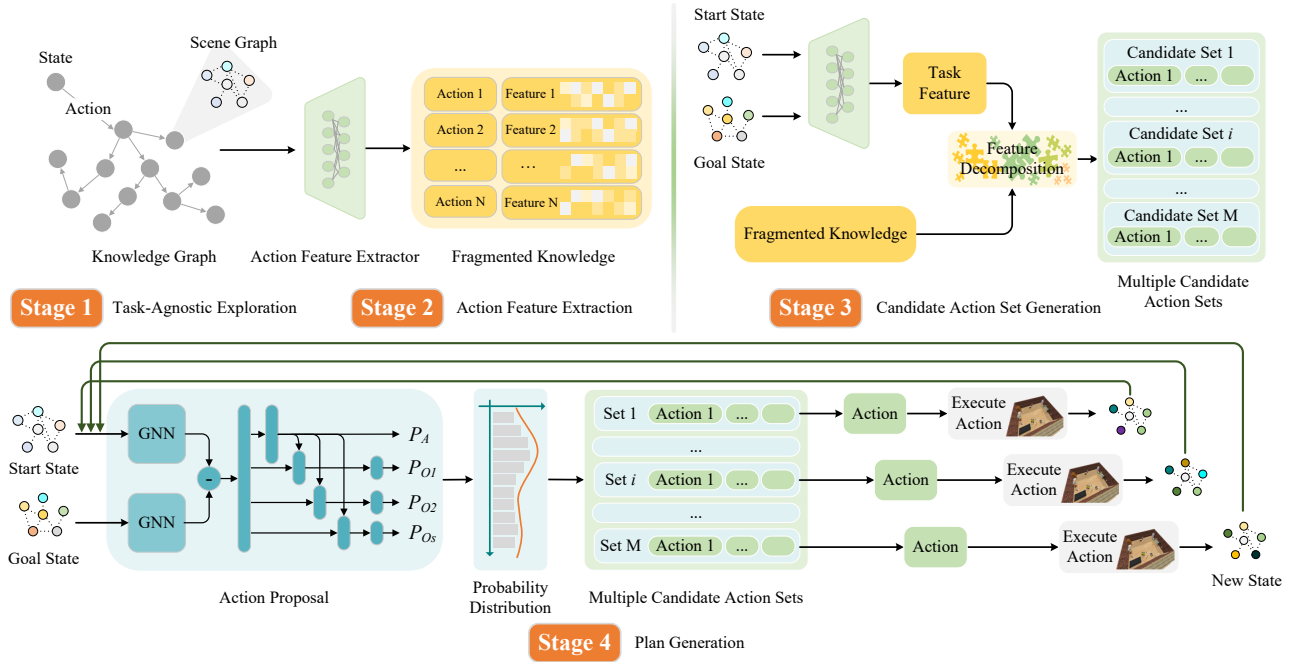


Fig. 1. The framework of TAL.

fixed goal, humans operate according to their curiosity. The meaningful action sequences collected in this way can be viewed as different skills. Play sequences are first sampled from the play data and encoded into the latent plan space. Then a goal-conditioned policy was trained to complete multiple tasks. Although this work achieves good performance, it is still limited to the patterns of goal-conditioned IL.

For IL methods, if expert demonstrations do not cover new tasks, their performance will deteriorate.

III. FRAMEWORK

The proposed TAL contains four stages. First, the task-agnostic exploration is performed to collect data from interactions with the environment. The collected data is organized via a knowledge graph. Second, an action feature extractor is proposed to learn task-agnostic fragmented knowledge. Third, a candidate action generator is designed to generate multiple candidate action sets for a new task. Finally, an action proposal is designed to generate the plan. The framework of TAL is shown in Fig. 1. In the following subsections, we will elaborate on the four stages respectively.

A. Task-agnostic Exploration

The task-agnostic exploration is performed to collect data from interactions with the environment. The collected data is organized via a knowledge graph.

1) *Knowledge Graph*: A knowledge graph: $\mathcal{G} = (\mathbb{S}, \mathbb{A})$ is built during environment exploration to collect data, where \mathbb{S} is the set of nodes and \mathbb{A} is the set of directed edges. A node $s_i \in \mathbb{S}$ represents an environmental state. An edge (s_i, s_j) is created if an action a_{ij} can be executed.

Previous works [54]–[57] typically employ a sequential structure to organize the explored data. Since the environment

is always initialized to the same or similar state, the sequence data may contain redundant fragments, making the exploration difficult. In contrast, we build a knowledge graph to organize the explored data. With the ability to restore the environment to various earlier states, the knowledge graph is more compact and makes it easier to explore the environment.

2) *Exploration*: At the start of the task-agnostic exploration, the node corresponding to the initial state of the environment is created, while the edge is an empty set. A round of exploration begins by randomly selecting a node s_i from \mathbb{S} . An action is then randomly sampled from the set of all executable actions. If the execution of the action fails, another action is sampled for execution. If the action can be executed successfully, a new node s_j is created to correspond to the new environmental state, and the edge from s_i to s_j is created. The next step of exploration starts from s_j . A round of exploration consists of several step explorations. Numerous rounds of exploration are carried out to sufficiently explore the environment. Finally, a knowledge graph with extensive data is built. The task-agnostic exploration is shown in Algorithm 1.

B. Action Feature Extraction

In this subsection, an Action Feature Extractor (AFE) is proposed to learn task-agnostic fragmented knowledge from the collected knowledge graph data. The action feature extraction is based on the states before and after an action is executed, which can be expressed as follows:

$$\mathbf{F}_{ij} = \text{AFE}(s_i, s_j | a_{ij}). \quad (1)$$

\mathbf{F}_{ij} is the action feature. s_i and s_j are environmental states before and after the action a_{ij} is executed. Next, we first

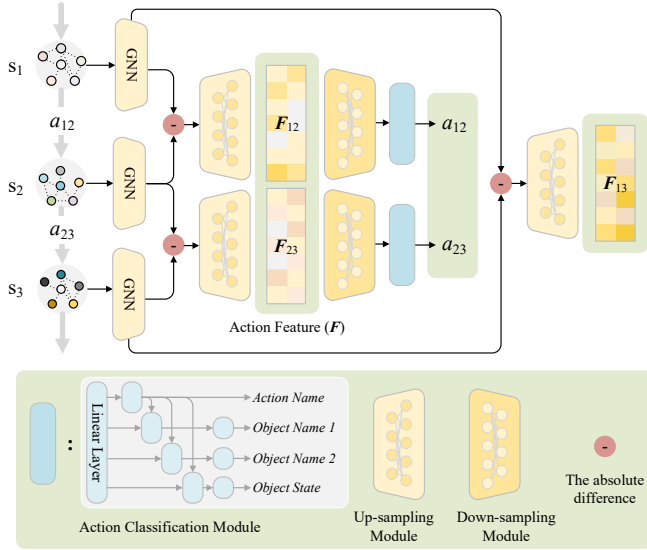


Fig. 2. The action feature extractor.

introduce the structure of AFE and then elaborate on the training strategy.

1) *Structure*: The structure of AFE is shown in Fig. 2. AFE takes the states before and after an action is executed as input, and outputs the action feature. AFE is made up of two Graph Neural Networks (GNNs) and one up-sampling module that is implemented by multiple linear layers. Each GNN captures one state feature from one input state. The absolute difference of the two captured state features is fed into the up-sampling module to extract the action feature. The action feature extracted by the up-sampling module is in a higher dimension space, therefore the features of different actions are more discriminative.

2) *Training Strategy*: In the following, we explain the training strategy in terms of training data and loss functions.

We sample paths of various lengths from the knowledge graph. The nodes (states) and edges (actions) in each path are extracted to form a trajectory. Trajectories are used to generate training samples. A training sample consists of three consecutive nodes and two edges between them. Next, we take a training sample $[s_1, a_{12}, s_2, a_{23}, s_3]$ as an example to introduce the training strategy. An action a_{ij} is represented by action name and parameters (object names and object state).

Due to the lack of supervised information for the training of AFE, an action classifier is introduced to guide the training of AFE. The classification labels supervise the training of the classifier and AFE. The action classifier can be represented as

$$\mathbf{T}_{ij} = \text{Classifier}(\mathbf{F}_{ij}). \quad (2)$$

\mathbf{T}_{ij} represents the predicted action tensor. \mathbf{F}_{ij} is the action feature. The action classifier consists of a down-sampling module and an action classification module, both of which are implemented by multiple linear layers.

AFE and the classifier are supervised by three loss functions.

$$\mathcal{L}_{AFE} = \mathcal{L}_{cls} + \mathcal{L}_f + \mathcal{L}_{add}. \quad (3)$$

Algorithm 1: Task-agnostic exploration

Output: A knowledge graph $\mathcal{G} = (\mathbb{S}, \mathbb{A})$

```

1 Initialize
2    $\mathbb{A}_{all}$  // The set of all executable actions.
3    $\mathbb{A} = \emptyset$  // The set of edges that represent actions.
4    $\mathbb{S} = \{s_0\}$  //  $s_0$  is the initial environmental state.
5 end
6 for  $round = 0$  to  $max\_round$  do
7    $s_i = \text{random\_select\_node}(\mathbb{S})$ 
8   for  $step = 0$  to  $max\_step$  do
9      $a = \text{random\_select\_action}(\mathbb{A}_{all})$ 
10     $success = \text{execute\_action}(a, s_i)$ 
11    while  $\neg success$  do
12       $a = \text{random\_select\_action}(\mathbb{A}_{all})$ 
13       $success = \text{execute\_action}(a, s_i)$ 
14    end
15     $s_j = \text{new\_state\_node}()$ 
16     $\mathbb{S} = \mathbb{S} \cup \{s_j\}$ 
17     $a_{ij} = \text{create\_edge}(s_i, s_j, a)$ 
18     $\mathbb{A} = \mathbb{A} \cup \{a_{ij}\}$ 
19     $s_i \leftarrow s_j$  // Next step starts from  $s_j$ .
20  end
21 end
    
```

The first loss function named action classification loss (\mathcal{L}_{cls}) ensures that extracted features are associated with actions. The second loss function named feature distinguish loss (\mathcal{L}_f) constrains the features of different actions to be more discriminative. The last loss function named additivity loss (\mathcal{L}_{add}) ensures the additive property of the action feature space.

\mathcal{L}_{cls} is calculated according to predictions of the classifier and action classification labels. For the training sample $[s_1, a_{12}, s_2, a_{23}, s_3]$, \mathcal{L}_{cls} is the sum of the prediction errors for the two actions.

$$\mathcal{L}_{cls} = \mathcal{L}_{bce}(\mathbf{T}_{12}, \mathbf{T}_{12}^*) + \mathcal{L}_{bce}(\mathbf{T}_{23}, \mathbf{T}_{23}^*). \quad (4)$$

Here, \mathbf{T}_{12} and \mathbf{T}_{23} are predicted action tensors of a_{12} and a_{23} respectively. \mathbf{T}_{12}^* and \mathbf{T}_{23}^* represent the ground truth tensors, which are the concatenation of the one-hot embeddings of action names and parameters. \mathcal{L}_{bce} represents the binary cross-entropy loss. Minimizing \mathcal{L}_{cls} ensures that extracted features are associated with actions.

\mathcal{L}_f is computed by the features of two actions. The loss function reduces the feature distance of the same action while increasing the distance between different actions.

$$\mathcal{L}_f = \begin{cases} 1 - \cos(\mathbf{F}_{12}, \mathbf{F}_{23}), & \text{if } a_{12} = a_{23} \\ \max(0, \cos(\mathbf{F}_{12}, \mathbf{F}_{23}) - \varepsilon), & \text{if } a_{12} \neq a_{23}. \end{cases} \quad (5)$$

\mathbf{F}_{12} and \mathbf{F}_{23} are the action features of a_{12} and a_{23} respectively. ε is a small offset. Minimizing \mathcal{L}_f constrains the features of different actions to be more discriminative.

\mathcal{L}_{add} is calculated according to three action features.

$$\mathcal{L}_{add} = \|(\mathbf{F}_{12} + \mathbf{F}_{23}) - \mathbf{F}_{13}\|_2^2. \quad (6)$$

Minimizing \mathcal{L}_{add} ensures the additive property of the action feature space.

AFE is trained end to end using the loss function \mathcal{L}_{AFE} .

C. Candidate Action Generation

In this subsection, a Candidate Action Generator (CAG) is proposed to generate a Candidate Action Set (CAS).

For a new task: T , representing the current environmental state as s_c and the goal state as s_g , the task feature F_T is extracted by AFE.

$$F_T = \text{AFE}(s_c, s_g). \quad (7)$$

The task feature reflects the environmental evolution, which is the superposition of the impacts of multiple actions taken to complete the task. According to the additive property of the feature space, the task feature can be decomposed into several action features which can be expressed as:

$$I_A F_A = F_T. \quad (8)$$

Here, $I_A \in \{0, 1\}^n$ is the action index corresponding to the actions in the action set \mathbb{A}_n . $\mathbb{A}_n = \{a_1, a_2, \dots, a_n\}$, a_i represents an action and n is the number of actions. $F_A = [F_1^T, F_2^T, \dots, F_n^T]^T$ is the features of actions in \mathbb{A}_n .

However, the action features are usually contaminated by noise, making Eq. (8) only approximately true.

$$\tilde{I}_A F_A = F_T. \quad (9)$$

\tilde{I}_A is an approximation of I_A .

To alleviate the impact of the noise, the Principal Component Analysis (PCA) is used.

$$F_A = U \text{diag}(S) V^T. \quad (10)$$

Then F_A and F_T are mapped into another feature space.

$$\tilde{I}_A F_A V = F_T V. \quad (11)$$

Finally, the action index is obtained as:

$$\tilde{I}_A = (F_T V)(F_A V)^+. \quad (12)$$

Here, superscript $+$ means the Moore-Penrose pseudo-inverse.

As \tilde{I}_A is an approximation of I_A , each element in \tilde{I}_A can be taken as the probability that an action will be used in the task. The actions corresponding to the *top-i* values of \tilde{I}_A are selected to form a CAS, denoted as \mathbb{A}_i ($\mathbb{A}_i \subseteq \mathbb{A}_n$).

For a new task, on the one hand, \mathbb{A}_i must contain as many correct actions as possible to solve the task. On the other hand, \mathbb{A}_i should contain as fewer incorrect actions as possible. Since an agent does not know how many acts are required when solving a new task, Multiple Candidate Action Sets (MCAS) are generated. Each CAS in MCAS contains a different number of actions, denoted as $\mathbb{M} = \{\mathbb{A}_i, \mathbb{A}_j, \dots, \mathbb{A}_k\}$.

D. Plan Generation by Action Proposal

This subsection generates the final plan to accomplish a new task. First, an action proposal is designed to produce the probabilities for actions according to the environmental information. Second, we generate the plan based on the probabilities.

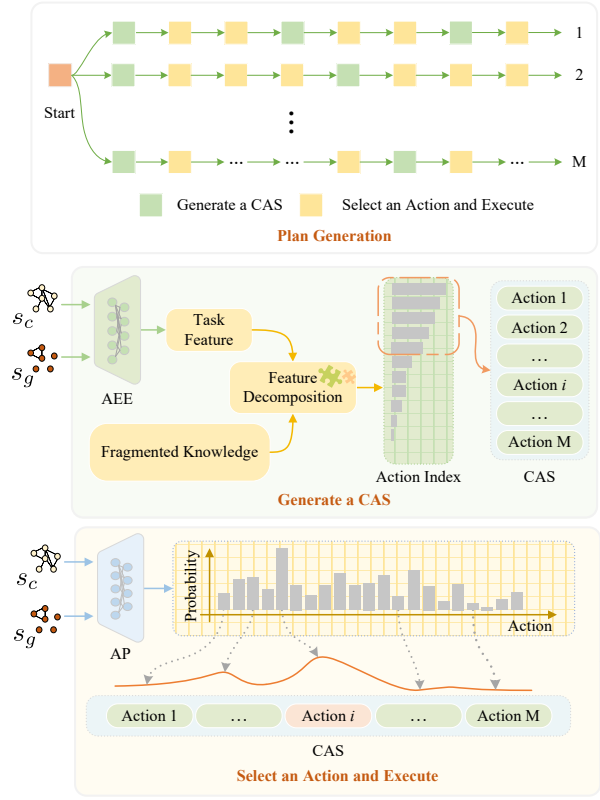


Fig. 3. Schematic diagram of the plan generation.

1) *Action Proposal*: Action Proposal (AP) is designed to generate the probability distributions for all executable actions which will be first executed for a new task from the current environmental state s_c to the goal state s_g . AP can be represented by

$$P = \text{AP}(s_c, s_g). \quad (13)$$

P consists of four probability distributions, corresponding to action name, object name 1, object name 2, and object state. Since the parameters (object name or state) are related to action name, similar to [58], AP first estimates action name and then the parameters. AP is formulated as follows:

$$\begin{aligned} P &= \text{concat}(P_A, P_{O_1}, P_{O_2}, P_{O_s}) \\ P_A &= \text{Softmax}(\text{MLP}_A(\mathbf{h}_1)) \\ P_{O_i} &= \text{Softmax}(\text{MLP}_{O_i}(\mathbf{h}_2)), \quad i = 1, 2, s \end{aligned} \quad (14)$$

where, $\mathbf{h}_1 = \text{PRReLU}(\text{MLP}_h(|\text{GNN}(s_c) - \text{GNN}(s_g)|))$, $\mathbf{h}_2 = \text{concat}(P_A, \mathbf{h}_1)$. Softmax and PRReLU are activation functions. MLP is a 3-layer perceptron. The GNNs used by s_c and s_g share weights. P_A is the predicted probabilities for action name, P_{O_1} and P_{O_2} are the predicted probabilities for object name 1 and object name 2, and P_{O_s} is the predicted probabilities for object state.

For an action in all executable actions, its probability is obtained by adding the four probabilities in P .

A binary cross-entropy loss is used to train AP. The label P^* consists of four parts, corresponding to P .

$$P^* = \text{concat}(P_A^*, P_{O_1}^*, P_{O_2}^*, P_{O_s}^*). \quad (15)$$

Here, $(P_A^*, P_{O_1}^*, P_{O_2}^*, P_{O_s}^*)$ are one-hot embeddings of the ground truth action.

AP is trained using the same dataset as AFE. For a training sample (s_i, s_g) in the training data $[s_1, a_1, s_2, \dots, s_g]$, its label is the one-hot embedding of the ground truth action a_i .

2) *Plan Generation*: The plan generation is shown in Fig. 3 and Algorithm 2. We take a CAS as an example to explain the plan generation. For a CAS, the plan is made up of ordered candidate actions. The order of actions is generated based on the probabilities generated by AP. For the current state s_c , the action with the highest probability in a CAS is executed, thus a new environmental state s_{new} is reached. AP takes s_{new} as s_c and repeats the previous iteration until all candidate actions have been executed.

Since a CAS may contain incorrect actions, early stopping is applied to avoid the wrong action execution, i.e., only the first several actions are executed. If the goal is reached, the plan generation process is terminated; otherwise, another CAS is generated by CAG based on the current and goal states. The task fails if a) the goal is still not reached after the maximum allowed step or b) some actions are not executed successfully, e.g., when the agent has something in its hand, it cannot pick up another object.

The plans for each CAS in MCAS are generated in parallel. From the perspective of ensemble learning, using MCAS still makes sense to improve performance.

For the whole plan generation process, we can think of a virtual environment as a human-generated scene in the brain. Actions are chosen in parallel from MCAS when processing a task and then executed simultaneously in multiple virtual environments. The generated plan is the result of brain thinking.

In addition, as some actions in a new task may not show in MCAS, i.e., never learned before, we use all executable action set \mathbb{A}_{all} to improve generality. The four parts of an action in \mathbb{A}_{all} are selected in turn according to their importance, i.e., $P_A \rightarrow P_{O_1} \rightarrow P_{O_2} \rightarrow P_{O_s}$. The plan generated based on \mathbb{A}_{all} is executed in parallel with plans of MCAS.

IV. EXPERIMENTS

In this section, we provide the experimental results of TAL and the comparison with the baselines. First, we introduce the experimental setup. Second, we explain the baseline settings. Third, we provide the experimental comparison. After that, ablation experiments are presented. Finally, discussions are provided.

A. Experimental Setup

1) *Environment*: We conduct the experiments with a virtual indoor scene [58] built in a physical simulator [45]. The environment contains a total of 35 objects. The mobile robot consists of a robotic arm (a Universal Robotics (UR5) arm) and a mobile base (a Clearpath Husky mobile base). The robot can perform a total of 11 actions such as “pick” and “drop”.

For the task-agnostic exploration, we modify the environment to improve the stability of the exploration. First, the robot may perform actions that are unusual in daily life during exploration, such as placing an orange on a water bottle.

Algorithm 2: Plan generation

Input: Current state s_c , goal state s_g
Output: Plans.

```

1 Initialize
2    $s_c = s_0$  //  $s_0$  is the initial state of a new task.
3    $F_A$  // Fragmented knowledge.
4    $F_T = AFE(s_c, s_g)$ 
5    $\{\mathbb{A}_i, \mathbb{A}_j, \dots, \mathbb{A}_k\} = \text{generate\_by\_CAG}(F_A, F_T)$ 
6    $max\_step = 60$ 
7 end
8 Parallel Execution
9   for  $\mathbb{A}_* \text{ in } \{\mathbb{A}_i, \mathbb{A}_j, \dots, \mathbb{A}_k\}$  do
10     $select\_num = 0, plan_* = [], success = \text{False}$ 
11    for  $step = 0$  to  $max\_step$  do
12     if  $select\_num > N_*$  then
13       $F_T = AFE(s_c, s_g)$ 
14       $\mathbb{A}_* = \text{CAG}(F_A, F_T)$ 
15       $select\_num = 0$ 
16     end
17      $a = \text{select}(\mathbb{A}_* | \text{AP}(s_c, s_g))$ 
18      $plan_* = plan_* + [a]$ 
19      $s_c = \text{execute}(s_c, a)$ 
20      $++select\_num$ 
21      $success = \text{check\_task}(s_c, s_{goal})$ 
22     if  $success$  then
23      break
24     end
25    end
26     $plan_* = plan_* + [success]$  // Add success flag.
27  end
28 end
29 return  $\{plan_i, plan_j, \dots, plan_k\}$ 

```

* N_* is the number for early stopping.

Therefore, we add constraints to avoid putting things on top of objects with uneven surfaces, such as bottles/apples/oranges. Second, the body of the robot may affect the result of the action, for example, by preventing objects from falling. We set the robot to back off a certain distance after acting as a push or placement to ensure the object falls. Third, to ensure that the current action is performed after the simulation of the previous action has ended, we set the simulation to end only when the displacements of all objects are less than a threshold. The modified environment details are shown in Table I.

2) *Dataset*: Three steps are performed to construct the dataset. The first step is to create the action set \mathbb{A}_{all} that contains all executable actions for environment exploration. The second step is to perform the task-agnostic exploration to build the knowledge graph. The third step is to generate the dataset from the knowledge graph.

In the first step, we combine different action names, object names, and object states to generate various actions. We finally get an action set with a total of 3598 actions. It is important to note that incorrect actions, such as “changeState <apple> <open>”, are filtered out by environmental feedback. The remaining 1364 actions after filtering form \mathbb{A}_{all} .

In the second step, the task-agnostic exploration is per-

TABLE I
ENVIRONMENT DETAILS

Action Names (11)	drop, climbDown, pick, moveTo, climbUp, pushTo, changeState, pickNplaceAonB, clean, apply, stick
Object Names (35)	floor, walls, door, fridge, cupboard, table, table2, couch, book, paper, cube_gray, cube_green, cube_red, tray, tray2, big-tray, bottle_blue, bottle_gray, bottle_red, chair, stick, box, apple, orange, dumpster, light, milk, shelf, glue, tape, stool, mop, sponge, vacuum, dirt
Object States (28)	Outside, Inside, On, Off, Close, Open, Up, Down, Sticky, Non_Sticky, Dirty, Clean, Grabbed, Free, Welded, Not_Welded, Drilled, Not_Drilled, Driven, Not_Driven, Fueled, Not_Fueled, Cut, Not_Cut, Painted, Not_Painted, Different_Height, Same_Height

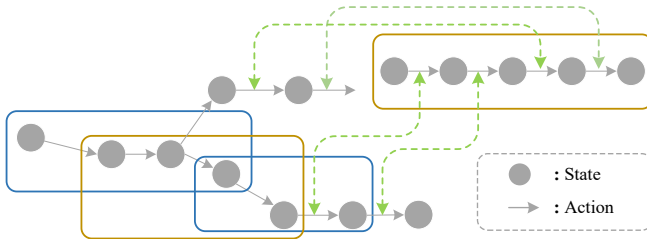


Fig. 4. Data schematic diagram. A blue rounded rectangle represents the training data, while a brown rounded rectangle is the test data. A green dotted line indicates the two same actions.

formed for knowledge graph generation. The whole process is shown in Algorithm 1. The *max_round* in the algorithm is set to 600. The *max_step* is set to 20 for the first round and 5 for the remaining rounds. In addition, the maximum number of attempts to explore the same node is set to 30. Finally, a knowledge graph is built with 2995 states and 855 different actions.

In the third step, the dataset is generated from the knowledge graph. We sample paths from the knowledge graph. In each path, the start node corresponds to the initial environmental state, and the end node is taken as the goal state of a task. The action sequence corresponding to the edges in each path is a solution plan. 300 paths with the same path length are sampled, and the path length (the number of edges in a path) ranges from 1 to 10, i.e., tasks required 1 to 10 actions to be completed. The generated dataset contains 3000 paths. We preferentially choose paths that have different endpoints and do not contain each other to increase the differences between paths.

The dataset is divided into three parts: training set, validation set, and test set. The training set is used to train AFE for fragmented knowledge learning and AP for generating the action proposal. The validation set is used to evaluate the model training and adjust hyper-parameters for better adaptation to new tasks. The test set is used to test the performance of the proposed TAL on new tasks. The training set, validation set, and test set are constructed by stratified sampling in a ratio of 6:2:2 for each path length, resulting in 1800 paths in the training set, 600 paths in the validation set, and 600 paths in the test set. Except for tasks that can be

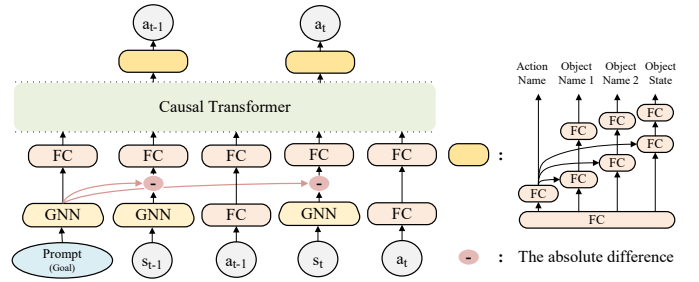


Fig. 5. Architecture of Prompt-plan Transformer.

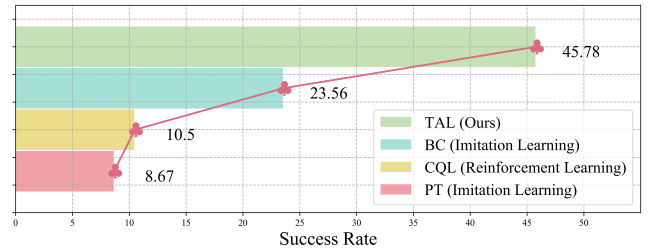


Fig. 6. Average performance comparison (R).

completed with one action, all tasks can be considered as new tasks, since they need new combinations of actions to reach their goal states. The data schematic diagram is shown in Fig. 4.

3) *Evaluation Metrics*: The evaluation metrics is the task success rate:

$$R = \frac{N_{success}}{N_{total}}. \quad (16)$$

R is the success rate. $N_{success}$ is the number of successful tasks, N_{total} is the total number of test tasks.

The criterion for judging whether the task is completed is related to the state of the environment and the state of the target. As suggested by [58], the criterion should satisfy some conditions: a) The comparison involves only task-related objects; b) Each task-related object must have a reference object for comparison; c) To consider the impact of various actions, the distance threshold for each action should be different.

4) *Implementation Details*: The textual data in the state is encoded by ConceptNet [59] to input to TAL. The optimizer is Adam with the default parameter settings in PyTorch. Each action feature’s size is initialized as 1×4096 and then reduced to 1×500 with PCA. The setting of MCAS is heuristic. We set it to contain 7 action sets. The action numbers and the number for early stopping in each set are [(5, 2), (10, 5), (15, 5), (20, 5), (20, 10), (30, 5), (30, 10)]. The maximum number of actions performed per task is set to 60. We use the proxy environment for testing [58]. The model training is accelerated using one NVIDIA GeForce RTX 2070 Super GPU.

B. Baselines

We introduce three baselines for comparison. The first method is the state-of-the-art model-free RL method called Conservative Q-Learning (CQL) [13]. The second method is

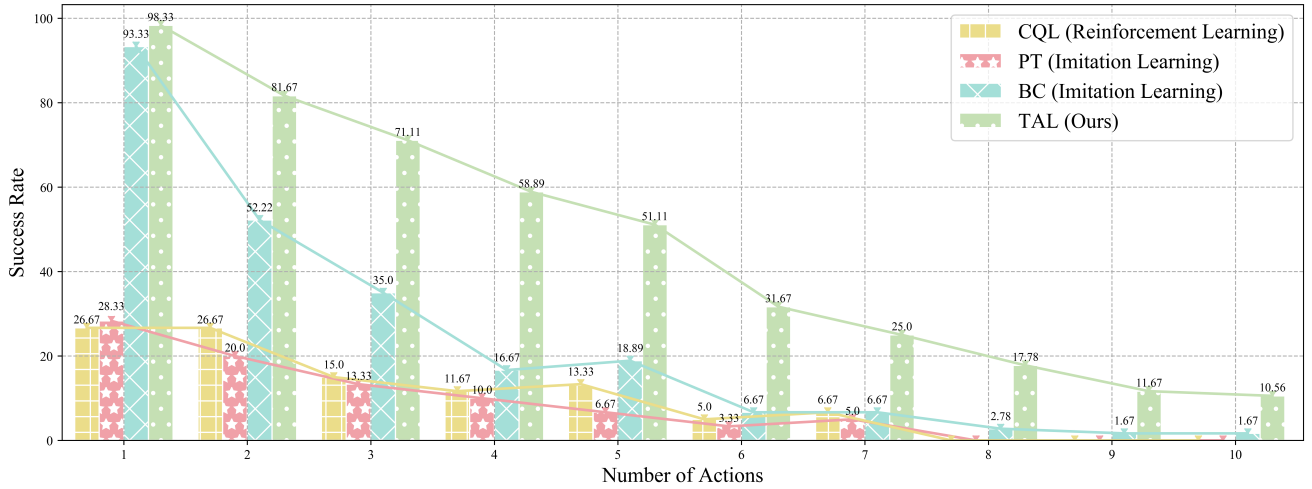


Fig. 7. Performance comparison (R) on 10 subsets of tasks that are required a different number of actions to complete.

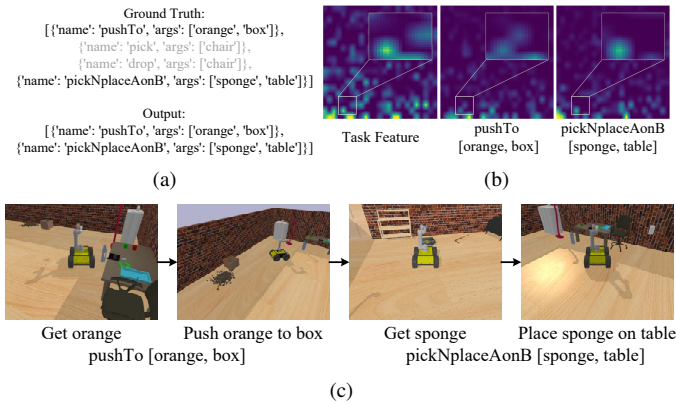


Fig. 8. An example task. (a) Ground Truth and output of our model. (b) Action feature visualization. (c) Execute the plan in the environment.

an IL method called Prompt-plan Transformer (PT), which is designed based on the transformer architecture [60]. The third method is a Behavioral Cloning (BC) method, which is also an IL method.

1) *CQL*: We set up the policy for CQL with the same architecture as AP (Section III-D), which estimates actions via feature differences between the current and goal states. According to the action's representation, The output consists of four Q-tables corresponding to action name, object name 1, object name 2, and object state. The policy is trained using the same training set as AFE and AP. In other words, the training set is taken as a fixed replay buffer.

All tasks are unified into a consistent form, which is generating action sequences that minimize the gap between the environmental state and the goal. We set the reward function by the Manhattan distance between the environmental state and the goal.

$$R_c(\mathbf{T}_c, \mathbf{T}_g, a_c) = \begin{cases} 1.0, & \text{if done (task completed)} \\ 1.0, & \text{if } L_1(\mathbf{T}_c, \mathbf{T}_g) < d \text{ and } a_c \in \mathbb{A}^* \\ 0.5, & \text{if } L_1(\mathbf{T}_c, \mathbf{T}_g) \geq d \text{ and } a_c \in \mathbb{A}^* \\ 0, & \text{if } a_c \notin \mathbb{A}^*. \end{cases} \quad (17)$$

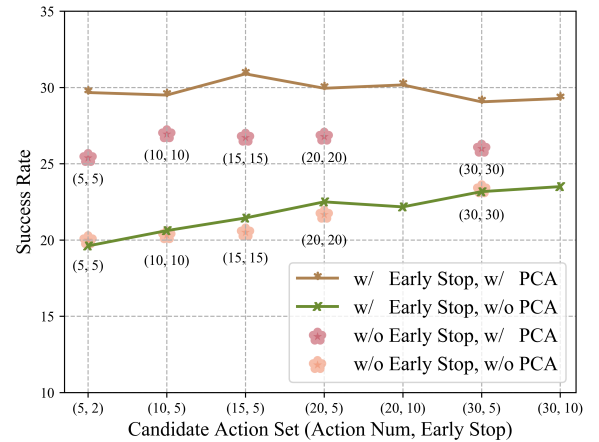


Fig. 9. Candidate action set analysis.

Here, d is the shortest distance between all previous states and the goal state. \mathbf{T}_c and \mathbf{T}_g are tensors composed of object information in current and goal states. \mathbb{A}^* represents the set of actions in ground truth plan. a_c is the current action predicted by the policy.

2) *PT*: We design PT based on the GPT architecture [60], as shown in Fig. 5. The inputs of PT are prompt (goal state), states, and actions in history. The output is an action for current execution. We feed the goal state to the network as a prompt so that PT can perform various tasks. The absolute difference between each input state and prompt is made at the feature level, so that PT pays more attention to the environmental change information. The causal transformer estimates each action only with the current and the previous environmental states, without considering the later ones. We set the maximum trajectory length of the model input to 5. The GNN structure and parameter settings are the same as AP. The same training set for AEF and AP is used to train PT. The loss function is the binary cross-entropy loss.

3) *BC*: As AP (Section III-D) can be taken as a behavioral cloning method, we use it for comparison.

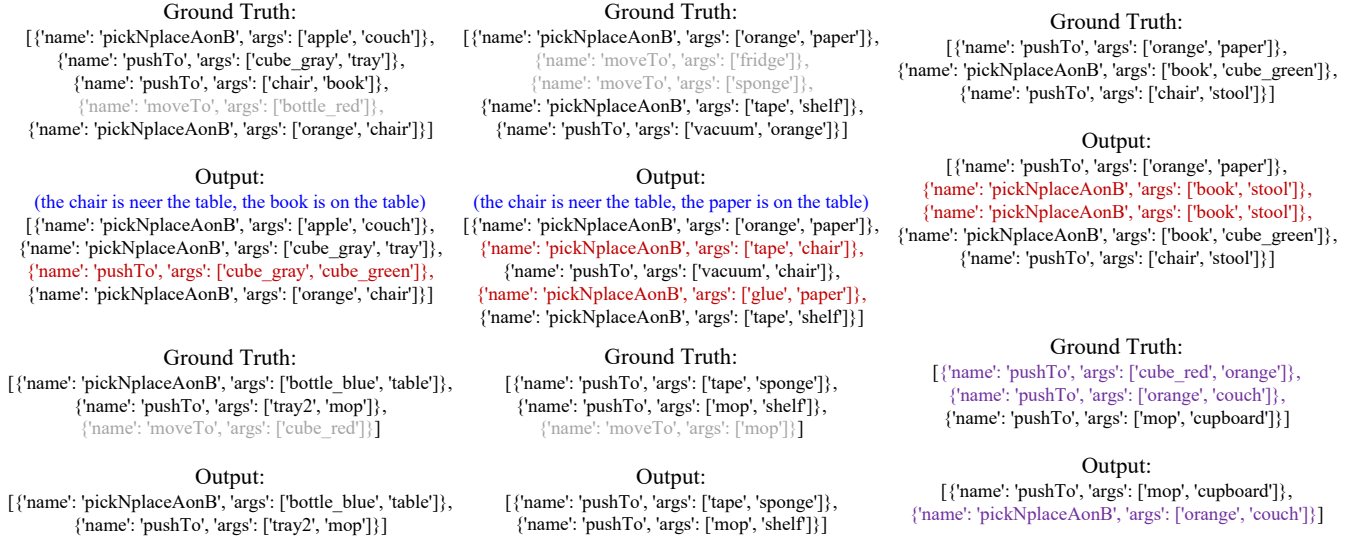


Fig. 10. Qualitative results. Gray indicates invalid operations, i.e., no changes to the environment. Red indicates incorrect actions. Blue is the description of the environment. Violet indicates knock-on impacts, where consecutive operations involve the same objects.

TABLE II
ABLATION EXPERIMENT RESULTS.

Setting					Average	Number of Actions									
Order	MCAS	Early Stop	PCA	A_{all}		1	2	3	4	5	6	7	8	9	10
\times	\checkmark	\checkmark	\checkmark	\checkmark	32.17	78.89	65.00	57.78	38.89	29.44	22.22	13.89	6.67	1.67	7.22
\checkmark	\times	\checkmark	\checkmark	\checkmark	33.00	93.33	72.22	56.67	38.33	31.67	15.56	10.00	7.22	0.56	4.44
\checkmark	\checkmark	\times	\checkmark	\checkmark	37.06	93.33	79.44	58.89	47.78	36.67	19.44	17.22	10.00	1.11	6.67
\checkmark	\checkmark	\checkmark	\times	\checkmark	36.83	98.33	79.44	63.89	38.89	31.67	19.44	11.67	9.44	5.00	10.56
\checkmark	\checkmark	\checkmark	\checkmark	\times	41.78	93.89	80.00	68.33	58.89	39.44	25.00	20.00	15.00	7.22	10.00
\checkmark	\checkmark	\checkmark	\checkmark	\checkmark	45.78	98.33	81.67	71.11	58.89	51.11	31.67	25.00	17.78	11.67	10.56

* "Number of Actions" is the number of actions in the ground truth plan. "Average" refers to the success rate of the whole test set. Bold indicates the best result.

C. Performance Comparison

The average success rates of compared methods on the entire test set are provided in Fig. 6. As can be seen, our TAL produces the highest success rate of 45.78%, which outperforms CQL by 35.28%, PT by 37.11%, and BC by 22.22%.

For a more detailed comparison, we split the test set into 10 subsets according to the number of actions required to complete tasks. The success rates of compared methods on each test subset are shown in Fig. 7. TAL achieves the highest average success rate on every test subset. The success rate of all models gradually decreases when the number of actions increases. PT and CQL have significantly lower success rates than TAL on each subset. For example, on task subset 2, TAL achieves a success rate of 81.67%, while BC, CQL, and PT drop to 52.22%, 26.67%, and 20.00%, respectively. On task subset 5, TAL has a success rate of 51.11%, while the success rates of BC, CQL, and PT are 38.38%, 13.33%, and 6.67%, respectively. On subset 7, TAL still has a 25% success rate, while the success rates of all other methods are less than 10%

Fig. 8 shows an example task and Fig. 10 displays some qualitative results. There are four situations involved in Fig.

10: a) The predicted plan has some incorrect actions; b) Ground truth plan contains invalid actions, such as just moving around without changing the state of other objects; c) The states of some objects already meet the task requirements; d) A knock-on impact occurs in ground truth plan, i.e., multiple different actions involve the same object. It can be seen that TAL provides good results for these new tasks.

D. Ablation Studies

A total of five ablation experiments are conducted, as shown in Table II. The first ablation experiment is performed to verify the role of the action execution order of MCAS. If "Order" is selected, actions in MCAS are executed according to the probability distribution generated by AP. If "Order" is not selected, actions in MCAS will be executed sequentially according to the action index \hat{A}_I (Eq. (12)). The second ablation experiment is conducted to verify the effectiveness of MCAS. We apply each CAS in MCAS for separate experiments and select the best result. The third ablation experiment is carried out to verify the rationality of early stopping. The settings of MCAS are [(2, 2), (5, 5), (10, 10), (15, 15), (20, 20), (30, 30)], indicating without early stopping. The fourth ablation

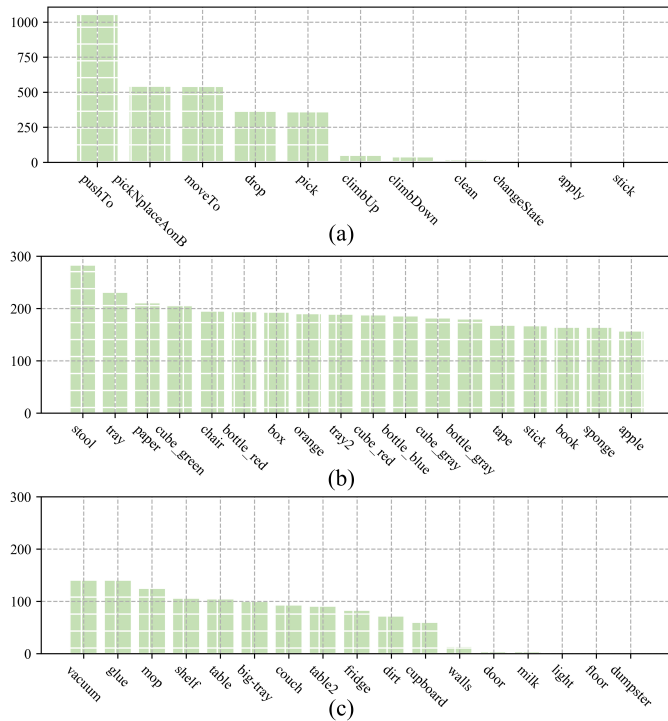


Fig. 11. The number of actions and object interactions performed in the dataset. (a) Action execution times. (b) Object Interactions (Part I). (c) Object Interactions (Part II).

experiment is provided to verify the effect of PCA. The last ablation experiment verifies the performance of using \mathbb{A}_{all} .

From Table II, we can see that “Order” and “MCAS” play the most important role. Using “Order” and “MCAS” results in 13.61% and 12.78% improvements in the average success rate respectively. “Early Stop” and “PCA” improve the average success rate by 8.72% and 8.95% respectively. “ \mathbb{A}_{all} ” contributes 4%.

Fig. 9 is an illustration to show the effectiveness of early stopping and PCA. In the line part, early stopping is applied, while the scatter part represents that it is not applied. In the case of not using PCA, the application of early stopping slightly improves the success rate. In the case of using PCA, early stopping significantly improves the success rate. Besides, whether with or without early stopping, PCA increases the success rate.

E. Discussions

In this subsection, we discuss two phenomena in the experiments. First, for failure tasks, the main reasons include: a) The task requires actions that the agent has not done before and b) For tasks that require long-term planning, error accumulation leads to failure. Second, we find the results of TAL at solving placement tasks are better than others. We analyze that this is related to how the environment is set up and how it is explored. Almost all objects in the scene can be paired with placement-related actions, but only a few objects can be combined with state-changing actions, as shown in Fig. 11.

These two phenomena indicate the importance of environment exploration. This will be extensively studied in the future.

V. CONCLUSION

In this paper, we propose a task-agnostic learning method (TAL for short) that can learn fragmented knowledge from task-agnostic data to accomplish new tasks. TAL consists of four stages. First, the task-agnostic exploration is performed to collect data which is organized via a knowledge graph. Second, the action feature extractor is proposed and trained using the collected knowledge graph data for task-agnostic fragmented knowledge learning. Third, the candidate action generator is proposed, which applies the action feature extractor on a new task to generate multiple candidate action sets. Finally, the plan generation is performed based on an action proposal. The experiments have confirmed the effectiveness of the proposed method on a virtual indoor scene.

REFERENCES

- [1] B. Singh, R. Kumar, and V. P. Singh, “Reinforcement learning in robotic applications: a comprehensive survey,” *Artificial Intelligence Review*, pp. 1–46, 2021.
- [2] H. Li, Y. Wu, M. Chen, and R. Lu, “Adaptive multigradient recursive reinforcement learning event-triggered tracking control for multiagent systems,” *IEEE Transactions on Neural Networks and Learning Systems*, 2021.
- [3] H. Li, Q. Zhang, and D. Zhao, “Deep reinforcement learning-based automatic exploration for navigation in unknown environment,” *IEEE Transactions on Neural Networks and Learning Systems*, vol. 31, no. 6, pp. 2064–2076, 2019.
- [4] H. Van Hasselt, A. Guez, and D. Silver, “Deep reinforcement learning with double q-learning,” in *Proceedings of the AAAI Conference on Artificial Intelligence*, vol. 30, no. 1, 2016.
- [5] G. Peng, C. P. Chen, and C. Yang, “Neural networks enhanced optimal admittance control of robot–environment interaction using reinforcement learning,” *IEEE Transactions on Neural Networks and Learning Systems*, vol. 33, no. 9, pp. 4551–4561, 2021.
- [6] Y. Keshnooloo, T. Shi, N. Ramakrishnan, and C. K. Reddy, “Deep reinforcement learning for sequence-to-sequence models,” *IEEE Transactions on Neural Networks and Learning Systems*, vol. 31, no. 7, pp. 2469–2489, 2019.
- [7] J. Schulman, F. Wolski, P. Dhariwal, A. Radford, and O. Klimov, “Proximal policy optimization algorithms,” *arXiv preprint arXiv:1707.06347*, 2017.
- [8] L. Zhang, R. Zhang, T. Wu, R. Weng, M. Han, and Y. Zhao, “Safe reinforcement learning with stability guarantee for motion planning of autonomous vehicles,” *IEEE Transactions on Neural Networks and Learning Systems*, vol. 32, no. 12, pp. 5435–5444, 2021.
- [9] T. G. Thuruthel, E. Falotico, F. Renda, and C. Laschi, “Model-based reinforcement learning for closed-loop dynamic control of soft robotic manipulators,” *IEEE Transactions on Robotics*, vol. 35, no. 1, pp. 124–134, 2018.
- [10] D. Hadfield-Menell, S. Milli, P. Abbeel, S. J. Russell, and A. Dragan, “Inverse reward design,” *Advances in Neural Information Processing Systems*, vol. 30, 2017.
- [11] J. Z.-Y. He and A. D. Dragan, “Assisted robust reward design,” in *Conference on Robot Learning*. PMLR, 2022, pp. 1234–1246.
- [12] S. Levine, A. Kumar, G. Tucker, and J. Fu, “Offline reinforcement learning: Tutorial, review, and perspectives on open problems,” *arXiv preprint arXiv:2005.01643*, 2020.
- [13] A. Kumar, A. Zhou, G. Tucker, and S. Levine, “Conservative q-learning for offline reinforcement learning,” *Advances in Neural Information Processing Systems*, vol. 33, pp. 1179–1191, 2020.
- [14] T. Yu, A. Kumar, R. Rafailov, A. Rajeswaran, S. Levine, and C. Finn, “COMBO: Conservative offline model-based policy optimization,” *Advances in Neural Information Processing Systems*, vol. 34, pp. 28 954–28 967, 2021.
- [15] D. Qin, A. Liu, J. Xu, W.-A. Zhang, and L. Yu, “Learning from human demonstrations for wheel mobile manipulator: An unscented model predictive control approach,” *IEEE Transactions on Neural Networks and Learning Systems*, 2022.

- [16] T. Zhang, L. Yue, C. Wang, J. Sun, S. Zhang, A. Wei, and G. Xie, "Leveraging imitation learning on pose regulation problem of a robotic fish," *IEEE Transactions on Neural Networks and Learning Systems*, 2022.
- [17] T. Osa, J. Pajarinen, G. Neumann, J. A. Bagnell, P. Abbeel, J. Peters *et al.*, "An algorithmic perspective on imitation learning," *Foundations and Trends® in Robotics*, vol. 7, no. 1-2, pp. 1–179, 2018.
- [18] C. Finn, S. Levine, and P. Abbeel, "Guided cost learning: Deep inverse optimal control via policy optimization," in *International Conference on Machine Learning*. PMLR, 2016, pp. 49–58.
- [19] J. Ho and S. Ermon, "Generative adversarial imitation learning," *Advances in Neural Information Processing Systems*, vol. 29, 2016.
- [20] F. Torabi, G. Warnell, and P. Stone, "Behavioral cloning from observation," in *Proceedings of the 27th International Joint Conference on Artificial Intelligence*, 2018, pp. 4950–4957.
- [21] K. Ehsani, S. Tulsiani, S. Gupta, A. Farhadi, and A. Gupta, "Use the force, luke! learning to predict physical forces by simulating effects," in *Proceedings of the IEEE/CVF Conference on Computer Vision and Pattern Recognition*, 2020, pp. 224–233.
- [22] V. Mnih, K. Kavukcuoglu, D. Silver, A. A. Rusu, J. Veness, M. G. Bellemare, A. Graves, M. Riedmiller, A. K. Fidjeland, G. Ostrovski *et al.*, "Human-level control through deep reinforcement learning," *Nature*, vol. 518, no. 7540, pp. 529–533, 2015.
- [23] T. P. Lillicrap, J. J. Hunt, A. Pritzel, N. Heess, T. Erez, Y. Tassa, D. Silver, and D. Wierstra, "Continuous control with deep reinforcement learning," *arXiv preprint arXiv:1509.02971*, 2015.
- [24] S. Fujimoto, D. Meger, and D. Precup, "Off-policy deep reinforcement learning without exploration," in *International Conference on Machine Learning*. PMLR, 2019, pp. 2052–2062.
- [25] S. Nair, S. Savarese, and C. Finn, "Goal-aware prediction: Learning to model what matters," in *International Conference on Machine Learning*. PMLR, 2020, pp. 7207–7219.
- [26] A. Campero, R. Raileanu, H. Kuttler, J. B. Tenenbaum, T. Rocktäschel, and E. Grefenstette, "Learning with AMIGo: Adversarially motivated intrinsic goals," in *International Conference on Learning Representations*, 2020.
- [27] R. Mendonca, O. Rybkin, K. Daniilidis, D. Hafner, and D. Pathak, "Discovering and achieving goals via world models," *Advances in Neural Information Processing Systems*, vol. 34, pp. 24 379–24 391, 2021.
- [28] M. Liu, M. Zhu, and W. Zhang, "Goal-conditioned reinforcement learning: Problems and solutions," *arXiv preprint arXiv:2201.08299*, 2022.
- [29] L. Mezghani, P. Bojanowski, K. Alahari, and S. Sukhbaatar, "Walk the random walk: Learning to discover and reach goals without supervision," in *ICLR Workshop on Agent Learning in Open-Endedness*, 2022.
- [30] M. Chevalier-Boisvert, L. Willems, and S. Pal, "Minimalistic gridworld environment for openai gym," 2018.
- [31] A. Gupta, V. Kumar, C. Lynch, S. Levine, and K. Hausman, "Relay policy learning: Solving long-horizon tasks via imitation and reinforcement learning," in *Conference on Robot Learning*. PMLR, 2020, pp. 1025–1037.
- [32] R. Devidze, G. Radanovic, P. Kamalaruban, and A. Singla, "Explicable reward design for reinforcement learning agents," *Advances in Neural Information Processing Systems*, vol. 34, pp. 20 118–20 131, 2021.
- [33] O. Wiles, S. Goyal, F. Stimberg, S. Alvisè-Rebuffi, I. Ktena, T. Cemgil *et al.*, "A fine-grained analysis on distribution shift," *arXiv preprint arXiv:2110.11328*, 2021.
- [34] B. Zheng, S. Verma, J. Zhou, I. W. Tsang, and F. Chen, "Imitation learning: Progress, taxonomies and challenges," *IEEE Transactions on Neural Networks and Learning Systems*, pp. 1–16, 2022.
- [35] A. Hussein, M. M. Gaber, E. Elyan, and C. Jayne, "Imitation learning: A survey of learning methods," *ACM Computing Surveys (CSUR)*, vol. 50, no. 2, pp. 1–35, 2017.
- [36] F. Torabi, G. Warnell, and P. Stone, "Recent advances in imitation learning from observation," in *IJCAI*, 2019.
- [37] C. Finn, P. Christiano, P. Abbeel, and S. Levine, "A connection between generative adversarial networks, inverse reinforcement learning, and energy-based models," *arXiv preprint arXiv:1611.03852*, 2016.
- [38] J. Merel, Y. Tassa, D. TB, S. Srinivasan, J. Lemmon, Z. Wang, G. Wayne, and N. Heess, "Learning human behaviors from motion capture by adversarial imitation," *arXiv preprint arXiv:1707.02201*, 2017.
- [39] Y.-H. Wu, N. Charoenphakdee, H. Bao, V. Tangkaratt, and M. Sugiyama, "Imitation learning from imperfect demonstration," in *International Conference on Machine Learning*. PMLR, 2019, pp. 6818–6827.
- [40] D. Garg, S. Chakraborty, C. Cundy, J. Song, and S. Ermon, "IQ-Learn: Inverse soft-Q Learning for imitation," *Advances in Neural Information Processing Systems*, vol. 34, pp. 4028–4039, 2021.
- [41] Z. Cao and D. Sadigh, "Learning from imperfect demonstrations from agents with varying dynamics," *IEEE Robotics and Automation Letters*, vol. 6, no. 3, pp. 5231–5238, 2021.
- [42] C. Finn and S. Levine, "Deep visual foresight for planning robot motion," in *2017 IEEE International Conference on Robotics and Automation (ICRA)*. IEEE, 2017, pp. 2786–2793.
- [43] P. Agrawal, A. V. Nair, P. Abbeel, J. Malik, and S. Levine, "Learning to poke by poking: Experiential learning of intuitive physics," *Advances in Neural Information Processing Systems*, vol. 29, 2016.
- [44] A. Edwards, H. Sahni, Y. Schroecker, and C. Isbell, "Imitating latent policies from observation," in *International Conference on Machine Learning*. PMLR, 2019, pp. 1755–1763.
- [45] E. Coumans and Y. Bai, "Pybullet, a python module for physics simulation for games, robotics and machine learning," 2016.
- [46] P. Sharma, D. Pathak, and A. Gupta, "Third-person visual imitation learning via decoupled hierarchical controller," *Advances in Neural Information Processing Systems*, vol. 32, 2019.
- [47] Z. Yang, K. Merrick, L. Jin, and H. A. Abbass, "Hierarchical deep reinforcement learning for continuous action control," *IEEE Transactions on Neural Networks and Learning Systems*, vol. 29, no. 11, pp. 5174–5184, 2018.
- [48] P. Dayan and G. E. Hinton, "Feudal reinforcement learning," *Advances in Neural Information Processing Systems*, vol. 5, 1992.
- [49] R. Parr and S. Russell, "Reinforcement learning with hierarchies of machines," *Advances in Neural Information Processing Systems*, vol. 10, 1997.
- [50] R. S. Sutton, D. Precup, and S. Singh, "Between MDPs and semi-MDPs: A framework for temporal abstraction in reinforcement learning," *Artificial intelligence*, vol. 112, no. 1-2, pp. 181–211, 1999.
- [51] T. G. Dietterich, "Hierarchical reinforcement learning with the MAXQ value function decomposition," *Journal of Artificial Intelligence Research*, vol. 13, pp. 227–303, 2000.
- [52] A. S. Vechnyevets, S. Osindero, T. Schaul, N. Heess, M. Jaderberg, D. Silver, and K. Kavukcuoglu, "Feudal networks for hierarchical reinforcement learning," in *International Conference on Machine Learning*. PMLR, 2017, pp. 3540–3549.
- [53] C. Lynch, M. Khansari, T. Xiao, V. Kumar, J. Tompson, S. Levine, and P. Sermanet, "Learning latent plans from play," in *Conference on Robot Learning*. PMLR, 2020, pp. 1113–1132.
- [54] D. Pathak, P. Agrawal, A. A. Efros, and T. Darrell, "Curiosity-driven exploration by self-supervised prediction," in *International Conference on Machine Learning*. PMLR, 2017, pp. 2778–2787.
- [55] Y. Burda, H. Edwards, A. Storkey, and O. Klimov, "Exploration by random network distillation," *arXiv preprint arXiv:1810.12894*, 2018.
- [56] A. P. Badia, P. Sprechmann, A. Vitvitskiy, D. Guo, B. Piot, S. Kapturowski, O. Tieleman, M. Arjovsky, A. Pritzel, A. Bolt *et al.*, "Never give up: Learning directed exploration strategies," in *International Conference on Learning Representations*, 2019.
- [57] R. Sekar, O. Rybkin, K. Daniilidis, P. Abbeel, D. Hafner, and D. Pathak, "Planning to explore via self-supervised world models," in *International Conference on Machine Learning*. PMLR, 2020, pp. 8583–8592.
- [58] S. Tuli, R. Bansal, R. Paul *et al.*, "TANGO: Commonsense generalization in predicting tool interactions for mobile manipulators," *arXiv preprint arXiv:2105.04556*, 2021.
- [59] R. Speer, J. Chin, and C. Havasi, "Conceptnet 5.5: An open multilingual graph of general knowledge," in *Proceedings of the AAAI Conference on Artificial Intelligence*, 2017.
- [60] A. Radford, K. Narasimhan, T. Salimans, I. Sutskever *et al.*, "Improving language understanding by generative pre-training,"